INTERNATIONAL JOURNAL OF PRECISION ENGINEERING AND MANUFACTURING Vol. 18, No. 12, pp. 1739-1748 DECEMBER 2017 / 1739

REGULAR PAPER

DOI: 10.1007/s12541-017-0202-5
ISSN 2234-7593 (Print) / 2005-4602 (Online)

# Evaluating the Performance of Kalman Filter on Elbow Joint Angle Prediction Based on Electromyography

**Triwiyanto Triwiyanto[1,3,#], Oyas Wahyunggoro[1], Hanung Adi Nugroho[1], and Herianto Herianto[2]**

1 Department of Electrical Engineering & Information Technology, Gadjah Mada University, Grafika No. 2, Yogyakarta, 55281, Indonesia
2 Department of Mechanical & Industrial Engineering, Gadjah Mada University, Grafika No. 2, Yogyakarta, 55281, Indonesia
3 Department of Electromedical Engineering, Health Polytechnic of Surabaya, Pucang Jajar Timur No 10, Surabaya, 60245, Indonesia
# Corresponding Author / E-mail: triwiyanto123@gmail.com, TEL: +62-08155126883

KEYWORDS: Kalman filter, EMG, Feature extraction, Zero crossing, Elbow joint prediction

*High accuracy in joint angle prediction is very important in the development of devices based on myoelectric control. Joint angle prediction based on a non-pattern recognition method is more preferred due to the robustness and the easiness to adapt to any subject. This paper proposed a new method to predict an elbow joint angle based on electromyography (EMG) which used a time domain feature, zero crossing, and Kalman filter. The EMG signals were collected from biceps muscle using Ag (AgCl) electrodes. To test the proposed method, the subjects were asked to move the elbow in the flexion and extension motion at different periods of motion (12 seconds, 8 seconds and 6 seconds). The EMG features yielded from the feature extraction step were processed using a Kalman filter which was used to predict an elbow joint angle. The performance of the proposed method was evaluated using root mean squared error (RMSE) and the Pearson's correlation coefficient (CC). In this study, the RMSE and CC values were ranged from 6.9o to 17.5o and 0.93 to 0.99 respectively. The results of the experiment have demonstrated the effectiveness of the proposed method to predict an elbow joint angle based on EMG signal.*

Manuscript received: September 19, 2016 / Revised: January 5, 2017 / Accepted: August 15, 2017

## 1. Introduction

Recently, electromyography (EMG) signals are widely used in a device based on a myoelectric control such as a prosthetic device and exoskeleton as an assistive or rehabilitative.[1,2] In addition to EMG signal, several studies used inertial,[3] accelerometer and gyroscope sensor[4,5] to track the movement of human limb. However, those mechanical sensors sensed only for current movement. Different to those mentioned sensors, the EMG signal is detectable for intended movement before the movement is executed.[6,7] Therefore, EMG signal is suitable to predict the position of the human limb. The accuracy of a predicted joint angle depends on an algorithm used in a prediction method. Some previous researchers[8,9] preferred to use a time domain features to extract the information in the EMG signals. Among the features, zero crossing (ZC) is the preferred feature to use because ZC could give frequency information. Dohony[10] reported that the elbow joint angle has a significant effect on the median frequency of the EMG signal. In ZC feature, there is a parameter (a threshold voltage value) that can be used to tune the accuracy of the predicted angle. Some studies[11–14] used ZC feature as an input for a classifier. Nevertheless, the previous researchers occasionally explored more in deep to perform the zero crossing feature. Feature extraction is commonly used as a pre-data processing in a joint-angle prediction algorithm. A properly selected feature determines the success of the classifier to predict a joint angle.

A joint prediction based on EMG signal is currently divided into two category[1] namely a pattern recognition and a non-pattern recognition based. Usually, joint-angle prediction algorithm is performed using a pattern recognition algorithm such as artificial neural network[9] (ANN), neuro-fuzzy[15,16] (NF) and support vector machine[17] (SVM). Although, they report a good accuracy in the predicted angle but a pattern recognition method needs a learning stage to train the network. A learning stage should be applied for each different subject so the system can recognize the EMG pattern. The learning stage would take time to implement the algorithm in the real time application. In some literature, a non-pattern recognition method is also applied to predict a joint angle. Joint angle is proportionally predicted based on EMG amplitude using a pre and post-processing with digital signal processing algorithm.

Jang[8] studied a model for a relationship between shoulder motion and the EMG signal. The model is performed using a spring damper pendulum with root mean square (RMS) as a feature extraction and a

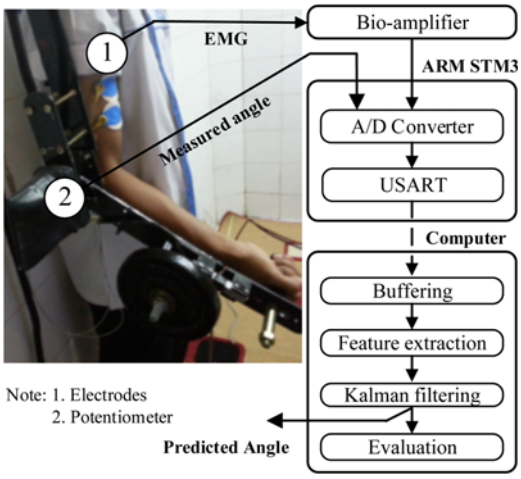


Fig. 1 Setup of data acquisition. The experimental setup consists of a bio-amplifier, a microcontroller and a standard personal computer

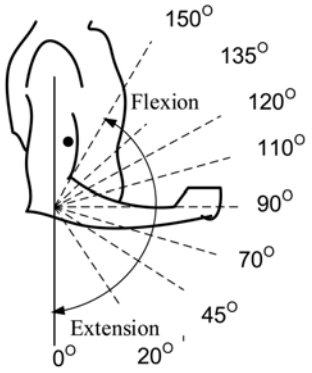


Fig. 2 Range of motion of the elbow joint angle in sagittal plane

low pass filter to cancel out the noise. However, the model needs to improve to minimize the ripple in the predicted angle. Lenzi[18] estimated a human muscular torque based on a human intention which was proportionally according to the EMG signal. Although he reported the results as a rough estimation, the system is a robust and does not need a calibration. To improve the performance of the prediction, some literatures discuss the combination of the pattern recognition and another method such as a Hill-based and a Kalman filter. Pau[19] developed a physiological model to predict an elbow joint angle. The prediction of joint angle is optimized using a genetic algorithm. Even though the model can predict the elbow joint angle with a low RMSE, the genetic algorithm cannot identify for a local minimum for complex movement trial. Kalman filter is commonly used by some previous studies[20-22] as a model to predict the force and the joint angle which is combined with a pattern recognition and a Hill-based method. However, Kalman filter used as an estimator model is not explored in depth.

Therefore, to fill the gap that has mentioned in the previous researchers, a new method needs to introduce to solve the problem in RMSE when the multiple cycles of movement are performed. Using a non-pattern recognition method will solve the problem in calibration when the subjects are changed. The aim of the proposed method is to predict an elbow joint angle using a zero crossing feature. To optimize the predicted angle, an estimator model is introduced using Kalman filter. The proposed method will not need a calibration procedure and training for the network.

## 2. Materials and Methods

### 2.1 Experiment protocol

In this study, four healthy male subjects were involved in the experiment. The subjects had no neuromuscular problem. Two disposable electrodes (Ag/AgCl, size: 57 × 48 mm, Ambu, Blue Sensor R, Malaysia) are placed at the biceps muscle in a differential configuration and one dry electrode as a common ground. The position of the electrode placement was according to Surface Electromyography for the Non-Invasive Assessment of Muscles (SENIAM) guidelines.[23] Biceps and triceps are related to flexion and extension motion respectively.[24] However, in the sagittal plane motion (flexion and extension), Lenzi proved that EMG signal collected from triceps muscle showed insignificant activities than that from biceps muscle.[18] Therefore in this study, the EMG signal was only collected from biceps muscle. As shown in Fig. 1 the subject wore an exoskeleton which consisted of two aluminum beam with a bearing in the elbow joint position. At the tip of the beam, a burden of two kg of load was placed. The subjects moved the elbow in flexion and extension direction of 0º to 150º (Fig. 2). The motion of the elbow was synchronized using a metronome application. The period of motion of the metronome was adjusted of 12 sec, 8 sec and 6 sec.

### 2.2 Data processing

The positions of the elbow joint were measured using a potentiometer (WX110-203, Bonens, China). The measured angle and EMG signal were sampled at frequency of 1,000 Hz. This rate has followed a Nyquist requirement.[25] Data acquisition consisted of a bio-amplifier, an internal A/D converter of ARM STM32 microcontroller, and a personal computer (Intel Core i3-3217U CPU at 1.80 GHz, 8 GB of RAM, Windows 8) for data processing. The bio-amplifier consisted of main instrumentation amplifier AD620 which is a low cost, a low power, a high accuracy amplifier and a high CMRR of 100 dB. ARMSTM32F429 was a high-speed microcontroller with 180 MHz clock which is fit for the requirement of the system. Data processing was conducted offline using a computer (Intel Core i3-3217U CPU at 1.80 GHz, 8 GB of RAM, Windows 8) and a Borland Delphi programming (Version 7.0, Borland Software Corporation, Scotts Valley, California, USA).

As shown in Fig. 3, the EMG signals were extracted using a zero crossing feature. $V_{threshold}$ was used to tune the output of the feature extraction. Kalman filter was used to estimate the best state of the predicted angle of the elbow joint. Kalman filter depended on some parameter which needed to be initialized in the modeling of Kalman filter. Those parameters were a noise measurement (R-parameter) and a noise process (Q-parameter).

#### 2.2.1 Feature extraction

Zero crossing feature is one of many time-domain features extraction used in an EMG signal analysis. Zero crossing is a number of time that

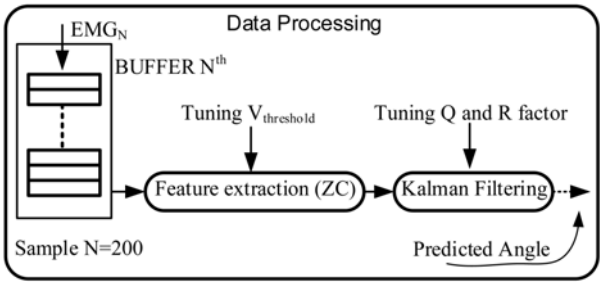


Fig. 3 Prediction algorithm of the elbow joint angle. Prediction algorithm is conducted off-line in a computer using a Delphi programming. Data processing consists of buffering data, a feature extraction and Kalman filter

the EMG signal crossed a baseline or a threshold value. The zero crossing can describe a frequency information in the EMG signal based on time domain. The previous researcher[10] has mentioned that the position of a joint such as an elbow and a knee affected the content of frequency of the EMG signals. Zero crossing feature was described as follow:[14,26-28]

$$ZC = \sum_{i=1}^{N-1} [sgn(x_i, x_{i+1}) \cap |x_i - x_{i+1}| \geq threshold]$$
$$sgn(x) = \begin{cases} 1, & if \rightarrow x \geq threshold \\ 0, & otherwise \end{cases} \quad (1)$$

where $x_i$ is the $i$-th sample, $N$ is the number of sample in each segment, *threshold* is the level of amplitude limitation and *sgn* is the sign function used to detect the position of the sample whether the sample is lower or higher than the threshold. The process of the feature extraction is shown in the Fig. 4. The explanation of Eq. (1) is implemented in the Algorithm 1.

**Algorithm 1:** Algorithm of the ZC feature

**Init**: $N = 200$; *threshold* = 0.12; $EMG_{ZC} = 0$;
**Input**: *EMG*[k]
**Output**: $EMG_{ZC}$
1. **FOR k** → 0 **TO** *N-1* **DO**
2. *sgn* = *EMG*[k] * *EMG*[k+1]
3. *diff* = **ABS** (*EMG*[k] - *EMG*[k+1])
4. **IF** (*sgn*> = *threshold* **AND** *diff* > = *threshold*)
5. **THEN** $EMG_{ZC} = EMG_{ZC} + 1$

End

where *EMG*[k] is the-*k* sample of the EMG signal, $EMG_{ZC}$ is the ZC feature extraction from 200 samples, *sgn* is a sign detection function and *diff* is a difference function which subtracts between two consecutive of samples *EMG*[k] and *EMG*[k+1].

In this study, the width of the window sampling was 200 samples and the threshold was selected between 80 and 200 mV based on experiment. This was due to each subject had different EMG characteristics.[29] Several studies had different threshold for the ZC feature. Hudgin[26] used threshold of 10 mV with a system gain of 5000 and Du et al.[30] applied threshold of 20 mV. Zardoshti et al.[31] predefined threshold between 50 and 100 mV.

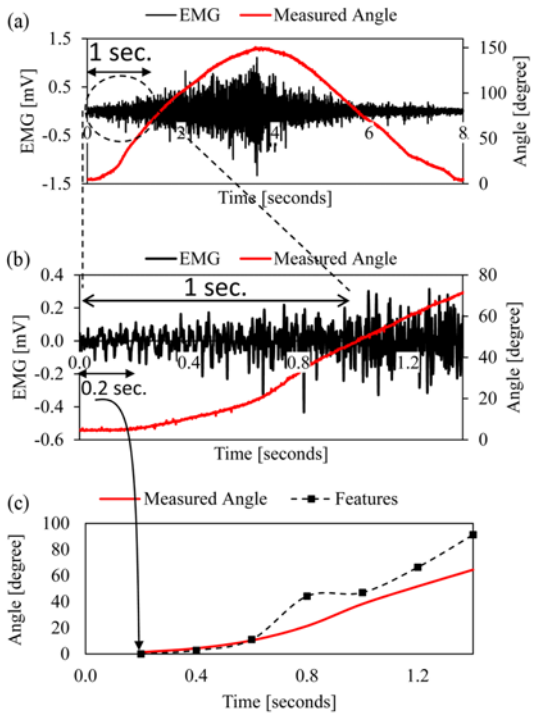


Fig. 4 Illustration of the feature extraction process of the EMG signals. (a) An EMG signals recording for one cycle of motion. (b) The EMG signals are extracted for every 200 sample (200 msec). (c) Feature extraction for 1000 msec. The red line is measured angles

### 2.2.2 Kalman filter

Kalman filter was first introduced by Rudolf Kalman[32] to solve the problem of the Winner work in a matter of filtering of the additive noise in the signals. Currently, Kalman filtering is used a lot in the field of navigation to predict the position of the object according to the last data information. Kalman filter is still a practical solution for digital signal processing problems. Kalman filter can perform an estimation[33] of the next state based on the previous state of the system and some parameters. The Kalman filter parameters, such as a process noise Q and a measurement noise R, need to be initialized with a certain value so the Kalman filter can perform with a good estimation.

Determination of the R and Q values was crucial which determined the performance of the Kalman filter. Practically, the R and Q values could be selected from any constant value which resulted an optimal prediction in the Kalman filter. Siswantoro et al.[34] selected the R and Q value in such way that it could improve the performance of the system. In this work, the R and Q values were selected based on experimental by choosing a positive real number. These parameters (R and Q) were needed to define for each subject during a tuning process to obtain the best performance of the prediction. This was due to the variability of the EMG signal that depended on the subjects.

In this paper, Kalman Filter estimated the predicted angle from the result of ZC feature extraction. The Kalman filter process is shown in Fig. 5. Assume the $x_k$ is the result of Kalman Filter prediction and $z_k$ is the resulted feature which can be expressed in a model of Eqs. (2) and (3).

$$x_k = Ax_{k-1} + Bu_k + w_k \tag{2}$$

$$z_k = Hx_k + v_k \tag{3}$$

where $x_k$ is a linear addition from the previous estimation $x_{k-1}$ plus a control input $u_k$ and a process noise $w_k$. $A$ is a transition matrix which relates current $x_k$ and previous estimation $x_{k-1}$. $B$ is a matrix which relates the current estimation $x_k$ and control input $u_k$. As shown in the Eq. (3), $H$ is a transition matrix which relates input measurement $z_k$ and estimation $x_k$ and $v_k$ is measurement noise.

The steps in Kalman Filter implementation are as follows:

**Step 1.** A prediction process consists of initial of a prior estimation and a prior error covariance. $\hat{x}_{k-1}$ is a prior estimate, which $\hat{x}_k^-$ is a temporary estimate before the correction step. Temporary error covariance $P_k^-$ is a linear addition between prior error covariance $P_{k-1}$ and a process noise $Q$, as written in the following equation:

$$\hat{x}_k^- = A\hat{x}_{k-1} + Bu_k + w_k \tag{4}$$

$$P_k^- = AP_{k-1}A^T + Q \tag{5}$$

**Step 2.** A Kalman gain $K_k$ was calculated from a temporary error covariance $P_k^-$ and a measurement noise $R$ as written in the following equation.

$$K_k = P_k^- H^T (HP_k^- H^T + R)^{-1} \tag{6}$$

**Step 3.** An update estimation $\hat{x}_k$ consists of a combination of a previous prior estimate $\hat{x}_k^-$ and differences between input measurement $z_k$ and a prior previous estimation $\hat{x}_k^-$ written as follow:

$$\hat{x}_k = \hat{x}_k^- + K_k(z_k - H\hat{x}_k^-) \tag{7}$$

**Step 4.** An update error covariance $P_k$ is a multiplication of a prior error covariance $P_k^-$ and Kalman gain $K_k$ written as follow:

$$P_k = (I - K_k H)P_k^- \tag{8}$$

The next step is iteration process which is the previous estimates and previous error covariance will be an input of the prediction stage, as shown in Fig. 5.

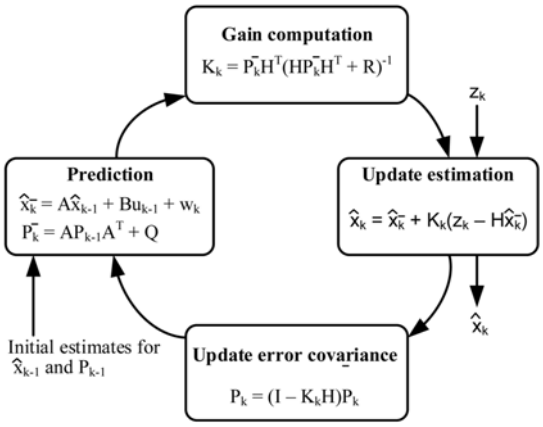


Fig. 5 Kalman filtering process

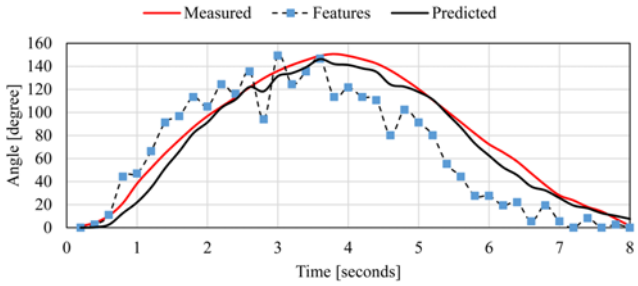


Fig. 6 Illustration of an elbow joint angle prediction using Kalman filter. The black line is the measured angle, the red line is the predicted angle and the thin line is the *EMG features* ($EMG_{ZC}$)

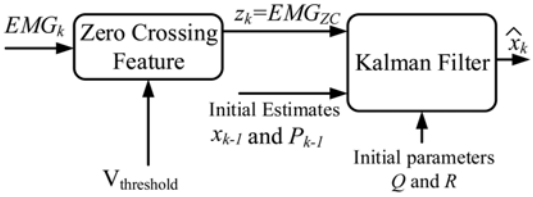


Fig. 7 The proposed method to predict an elbow joint angle. A combination algorithm of zero crossing feature and Kalman filter

An illustration that describes a Kalman filter process is shown in Fig. 6. The features ($EMG_{ZC}$) which are yielded from the feature extraction process show some random values but the feature follows the measured angle. Kalman filter used $EMG_{ZC}$ as input of the Kalman filter ($z_k$) to update a new estimation which was assigned as $\hat{x}_k$ In a modeling Kalman filter, the output of the Kalman filter, the predicted angle, depended on a process noise (Q) in the prediction step and a measurement noise (R) in gain computation step.

### 2.3 Proposed method

Assuming a Kalman filter is used to predict an elbow joint angle as in Fig. 7. EMG features $EMG_{ZC}$ resulted from feature extraction process are used as input of Kalman filter $z_k$.

The proposed method consists of two processes, which is a feature extraction and a prediction process. The processes of the feature extraction are as follows (Fig. 7): defining a certain threshold value, extracting EMG signal for each 200 number of sample point using zero crossing feature. The processes of the prediction are as follows: defining a constant value for Q and R parameters, expressing an initial estimate $\hat{x}_{k-1}$ and initial error covariance $P_{k-1}$, calculating the prediction of a prior state and an error covariance, computing the Kalman gain, updating the estimation state according to current measurement $z_k$. Since the state of the signal does not change from time to time, the element matrix of $A$, $B$ and $H$ is thus assumed as a constant and equal to one. According to Eqs. (2) and (3), a linear model of Kalman filter is modified as follow:

$$x_k = x_{k-1} + u_k + w_k \tag{9}$$

$$z_k = x_k + v_k \tag{10}$$

where, $x_k$ is current estimation, $x_{k-1}$ is prior estimation, $w_k$ is a process noise with covariance Q and $v_k$ is a measurement noise with covariance R. Since, there is no control parameter $u_k$ in the EMG signal therefore Eq. (9) can be expressed as follow:

$$x_k = x_{k-1} + w_k \tag{11}$$

A linear model Kalman filter for one dimensional based on previous equation Eqs. (4) to (8) is written as follow:

**Step 1**. A prediction stage

$$\hat{x}_k^- = \hat{x}_{k-1} \tag{12}$$

$$P_k^- = P_{k-1} + Q \tag{13}$$

**Step 2**. Kalman gain computation

$$K_k = P_k^-(P_k^- + R)^{-1} \tag{14}$$

**Step 3**. Update estimation

$$\hat{x}_k = \hat{x}_k^- + K_k(z_k - \hat{x}_k^-) \tag{15}$$

**Step 4**. Update error covariance

$$P_k = (I - K_k)P_k^- \tag{16}$$

In this study, the algorithm of the proposed method was implemented using Delphi programming (Version 7.0, Borland Software Corporation, Scotts Valley, California, USA). Flowchart of the proposed method is shown in the Fig. 8. The collected EMG data, which contain a time series of the EMG signal and the measured angle, were opened and plotted in a chart to visualize the pattern of the signal and the real angle. Before calculating the feature extraction and Kalman filtering, some parameter needed to be defined such as, threshold voltage, number of sample, R and Q parameters.

### 2.4 Statistical analysis

The statistical analysis was performed using Microsoft Excel with an add-insert toolbox (real statistics) from real-statistics.com. The performance of the prediction was evaluated using the root mean square error (RMSE) as mentioned in some literatures.[9,19,22,35,36] The RMSE value could describe the accuracy of the prediction algorithm. Some previous researchers[9,14,22,36] used the Pearson's correlation coefficient to measure the strength of a linear relationship between the predicted angles and the measured angles. Variability of the RMSE between and within the subjects was described using a boxplot diagram. A single-factor analysis of variance (ANOVA)[37] was conducted to test the null hypothesis. In this study, the null hypothesis was there were no differences of RMSE between the subjects. The analysis was used to see whether there were no differences of the mean RMSE between subjects. An F-value was used as a threshold value to decide if the null hypothesis is rejected or fail to reject. When the F-value is less than a $F_{critical}$-value then we accept the null hypothesis. The significant difference of the mean RMSE between subjects (subject: A, B, C and D) was tested using a p-value with the level of confident of 95% (alpha = 0.05). When the p-value is higher than an alpha value, then it indicates that there is no significant difference of mean RMSE between the subjects.

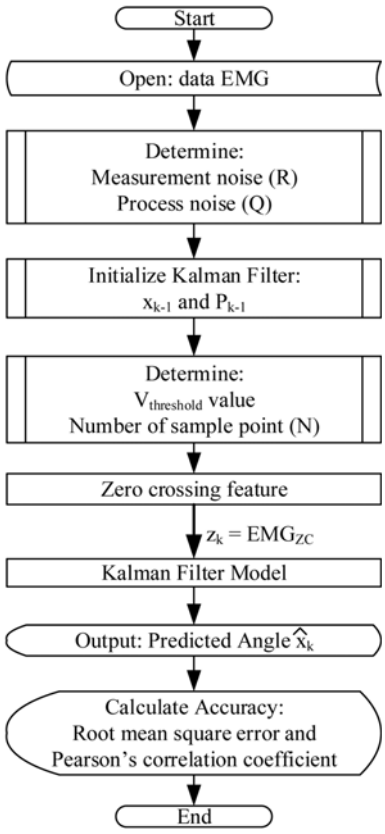


Fig. 8 Flow chart of proposed method for feature extraction and Kalman filtering process. Performed offline using Delphi programming

## 3. Results

The results have demonstrated the effectiveness of the proposed method to predict an elbow joint angle using EMG signal. The accuracy of the predicted angle was varied with ranged from 6.9° to 17.5° and there was a high relationship between the predicted angle and the measured angle which the Pearson's correlation coefficients were 0.93 to 0.99.

The EMG signals (Fig. 9(a)) were recorded from biceps muscle. The real positions of the elbow joint were measured using a linear potentiometer sensor. The range of motion of the elbow joint (in flexion and extension) was approximately 0 to 150 degrees as shown in Fig. 9(a). The elbow was moved in the flexion and extension continuously for 5 cycles. Each 200 sample of point (sampling frequency of 1,000 Hz), the EMG signals were extracted using a zero crossing feature (Fig. 9(b)). A threshold voltage value was set to a certain value (0.08-0.2 V) as shown in Eq. (1). A threshold value was adjusted according to the

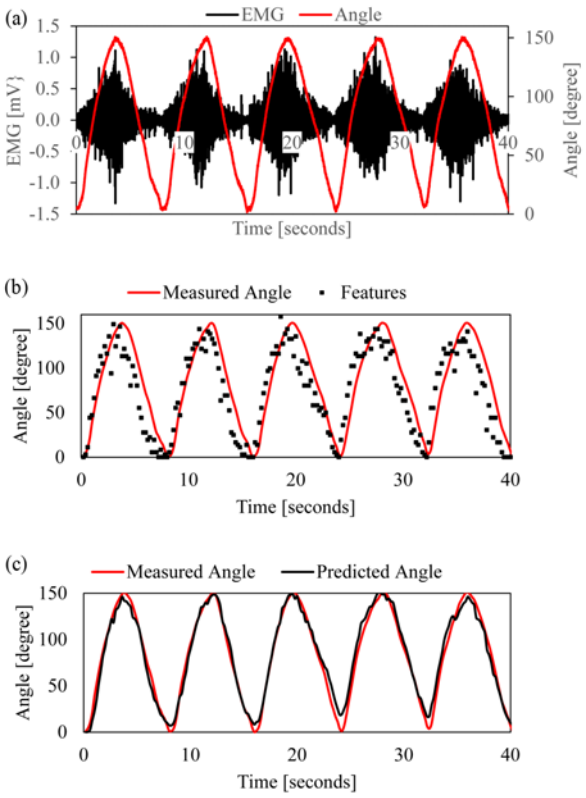


Fig. 9 (a) The raw EMG signal. The right axes is the position of the measured angle. The left axes is the EMG amplitude (b) Feature extraction. (c) Predicted angle. The red line is the measured angle and the black line is the predicted angle. Sample from subject B

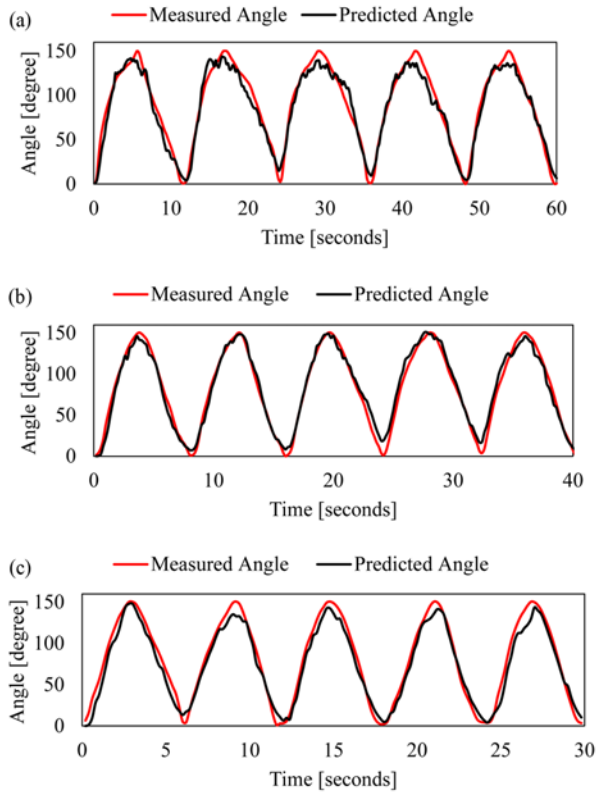


Fig. 10 The predicted and measured angles of five continuous cycles. Movement of the elbow joint on the period of motion at (a) 12 second. (b) 8 second and (c) 6 second. The black line is the predicted angles which are the result of our proposed method and the red line is the measured angles. Sample from subject B

nature of the EMG signal which depends on subjects. In Fig. 9(b), the features of the EMG signals were expressed as a cross symbol. The pattern of the features almost coincided with the measured angle but the RMSE value was large enough at 31.42° and the correlation coefficient at 0.84. The proposed method was used to reduce the error in the prediction that resulted from the feature extraction step and to increase the linear relationship between the predicted and the measured angle. Fig. 9(c) shows the predicted angle denoted by the black line. The predicted angles are improved after processing the feature extraction using the Kalman filter algorithm.

Some parameters of the Kalman filter, such as a measurement noise (R) and a process noise (Q), were needed to be initialized with a certain value. Those parameters were very important to determine the accuracy of the prediction. The predicted angles showed in the Fig. 9 (c) are that used Q and R value of 0.04 and 0.6 respectively.

The proposed method was tested with a different period of motion (12 sec, 8 sec and 6 sec) to verify that the system could perform well in the different speed of motion (Fig. 10). The effectiveness of the proposed method was tested using root mean square error and Pearson's correlation coefficient. The RMSE values were calculated each cycle during five continuous cycles for each subject (A, B, C and D) to observe the variance between subjects. As shown in Fig. 11 and Table 1, for all subjects (A, B, C and D), the average of the mean RMSE for periods of motion 12 sec, 8 sec and 6 sec were 12.95 1.99, 11.86 1.86 and 12.96 1.60 respectively. The average of the maximum RMSE for periods of motion 12 sec, 8 sec and 6 sec were 16.46 2.25, 15.29 2.32 and 17.26 0.67 respectively. The average of the minimum RMSE for periods of motion 12 sec, 8 sec and 6 sec were 9.57 2.03, 8.19 1.06, and 8.67 2.36 respectively. The average of the Pearson's correlation coefficient between the predicted angle and the measured angle was

Table 1 Summary of mean and standard deviation of RMSE and Pearson's correlation coefficient (CC) for subjects A, B, C and D at different period of motion

| Period of Motion [sec] | Subject | RMSE [deg] (Mean ± SD) | CC (Mean ± SD) |
|---|---|---|---|
| 12 | A | 11.510 ± 3.307 | 0.983 ± 0.01 |
| | B | 13.505 ± 4.177 | 0.967 ± 0.03 |
| | C | 14.267 ± 1.969 | 0.973 ± 0.004 |
| | D | 11.010 ± 2.193 | 0.986 ± 0.004 |
| 8 | A | 13.086 ± 3.119 | 0.978 ± 0.005 |
| | B | 9.414 ± 2.530 | 0.991 ± 0.004 |
| | C | 13.507 ± 3.385 | 0.971 ± 0.015 |
| | D | 11.430 ± 2.825 | 0.985 ± 0.005 |
| 6 | A | 13.114 ± 4.160 | 0.971 ± 0.015 |
| | B | 11.169 ± 4.422 | 0.986 ± 0.007 |
| | C | 12.517 ± 3.791 | 0.984 ± 0.008 |
| | D | 15.027 ± 2.137 | 0.959 ± 0.013 |

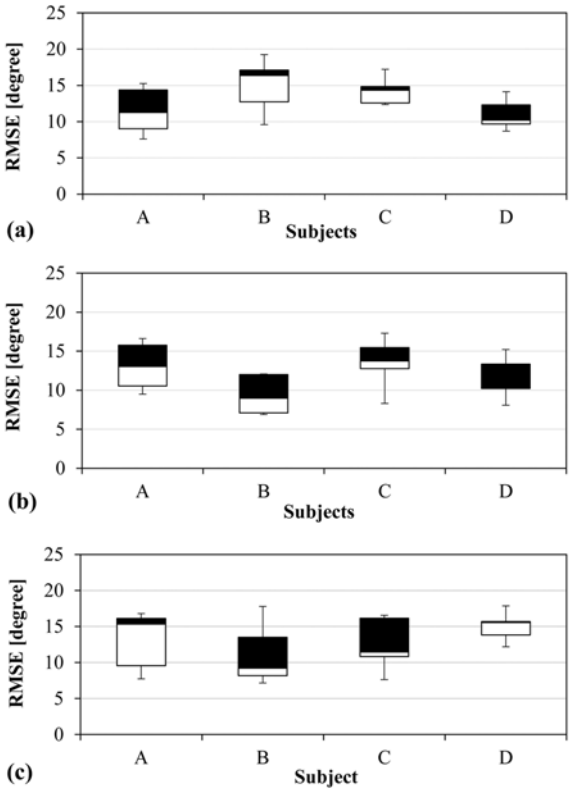


Fig. 11 The comparison of the RMSE boxplot during continuous cycles for periods of motion at (a) 12 sec, (b) 8 sec and (c) 6 sec. Each subject (A, B, C and D) performs the motion in the three different periods. The left axes indicate the RMSE values in degrees

Table 2 Summary of F-values and p-values of ANOVA from the period of motion of 12 sec, 8 sec and 6 sec. Each period of motion is conducted by subject A, B, C and D. Level of confidence in 95% (alpha = 0.05)

| Period of motion | F | F-critical | p-value |
|---|---|---|---|
| 12 sec (subject A, B, C, D) | 1.314 | 3.239 | 0.304 |
| 8 sec (subject A, B, C, D) | 1.946 | 3.239 | 0.163 |
| 6 sec (subject A, B, C, D) | 0.920 | 3.239 | 0.453 |

Note: $H_0 = \mu_A = \mu_B = \mu_C = \mu_D$ (There is no significant different between subjects and periods)

0.978 0.003 for all of the period of motion and all of the subjects.

ANOVA was used to examine whether there is significant difference or not between the subjects for the same period. Table 2 shows that all of the F values are lower than the F-critical (F-critical > F) and all of the p-values are higher than the alpha (p-value > alpha).

The performance of the proposed method depended on Kalman filter initialization. In this study, we performed an experiment on the Kalman filter parameters, those are a process noise (Q) and a measurement noise (R). Fig. 12(a) shows the accuracy (RMSE) of the predicted angle which was tested with several Q-parameter values in the range of 0.01 to 0.2. As shown in Fig. 12(a), when the Q-parameter is equal to 0.03 then the RMSE is the lowest value (RMSE = 7.00°) on the period of motion of

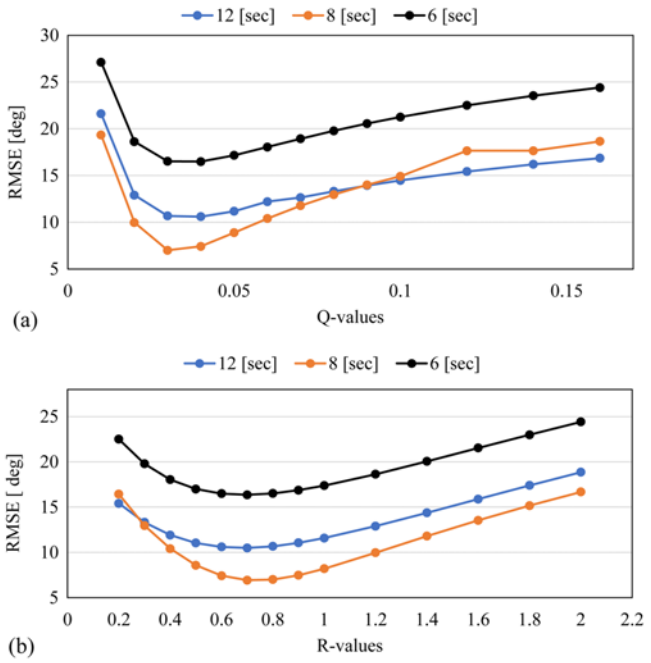


Fig. 12 The effect of (a) Q and (b) R parameter in the RMSE. The dotted line denotes the trend line of the fourth order of polynomial function

8 seconds. The accuracy of Kalman filter model was also tested with some values of a parameter of R within the range of 0.2 to 2. As shown in Fig. 12(b), the lowest value of the RMSE is when the R parameter is equal to 0.7 (RMSE = 6.9°). According to Figs. 12(a) and (b), the RMSE value is the lowest when the flexion and extension motion are in the period of 8 seconds.

## 4. Discussion

Our proposed method has demonstrated the effectiveness of the Kalman Filter to predict an elbow joint angle. We found that the Pearson's correlation coefficient average is 0.978 0.003 which means there is a high relationship between the predicted and measured angles for three different periods of motion and subjects. The average of the mean RMSE for a period of motion of 12 sec, 8 sec and 6 sec is 12.95° 1.99°, 11.86° 1.86° and 12.96° 1.60° respectively. Similar results are also reported by Tang[9] that the RMSE for three different periods of 8 sec, 4 sec and 2 sec are 12.42°, 9.67° and 10.70° respectively. He developed the model using an artificial neural network and tested for a single subject. The model proposed by Pau[19] reported that the RMSE is 22.00° ± 6.6° for five continuous cycles but he found the accuracy of 6.53° for a single cycle. Koo[38] reported that the average RMSE is 34.64 ± 7.79°. Lee[39] estimated a joint angle trajectory using total co-contraction level or joint stiffness for four different kinds of lifting speed. He measured the predicted angle using correlation coefficient, which were ranged from 0.698 ± 0.03 to 0.92 ± 0.018.

A minimal number of the EMG channel used to predict an elbow joint angle is essential for feasibility to apply in the real life. In this study, EMG signal from a biceps muscle is used to perform an elbow

joint angle prediction with good accuracy as mentioned in Table 1. Previous researchers used two muscles (biceps and triceps) to predict an elbow joint angle and the others used more than two muscles. According to the physiology and anatomy literature[24] the biceps muscle is only responsible for the action of the elbow flexion. In accordance with the flexion and extension motion in this study, while the elbow in an extension motion the biceps muscle may still retain the force of the gravity, therefore EMG signal still exists in the extension motion.

According to Table 2 (F < F-critical and p-value > alpha), the statistic suggests that we fail to reject the null hypotheses and there are no significant differences of the RMSE between the period of motion and subjects. This demonstrates that the proposed method works well for all of the subjects and periods of motion.

Q and R parameters in the Kalman filter affect the performance of the proposed method. For the three different periods of motion (subject B), we found that the RMSE is lowest when the Q-value and the R-value are 0.03 and 0.7 respectively (Fig. 12). Q and R parameters are not a linear function to affect the performance of the proposed method but approach to a fourth-order polynomial function. We suggest that the Q-value and the R-value for the Kalman filter parameters can be adjusted according to Fig. 12 to get the best RMSE.

The results obtained from this study are very promising to be applied in the same research area, such as exoskeleton devices and prosthetic devices. The proposed method is categorized as a non-pattern recognition method therefore it does not need time for learning the process. The adaptation to this system is adjusting the Q and R parameters which are defined in the Kalman filter algorithm.

There are many factors that may affect the EMG signal which are not considered in this study such as muscle fatigue, electrode position and acceleration of motion. It is a common problem in daily life when the part of our body does an intensive and repetitive activity then we will experience a fatigue condition since the muscle cannot maintain the force. According to Basmajian and De Luca,[40] the mean power frequency of the EMG signal will shift to the left (decreasing) and EMG amplitude tends to increase when the muscle fatigue is induced. In conjunction with this study, the muscle fatigue will change the output of the feature extraction and affect the prediction algorithm. In the next work, it needs a new algorithm to compensate the muscle fatigue effect so that the performance of the proposed method can be maintained.

## 5. Conclusion

In this study, we prove the effectiveness of the proposed method to predict an elbow joint angle using a zero crossing feature and optimize the feature using a Kalman filter. A single channel of EMG signal, generated from biceps muscle, is used to predict an elbow joint angle. The proposed method is tested using four subjects and three different periods of motion to evaluate the reliability of the system. The results show that there are no significant differences of the mean RMSE for different periods and subjects. The Q and R Parameters of the Kalman filter affect the RMSE of the proposed method, therefore the right choice of the parameter values is needed. Many factors may affect the EMG signal such as muscle fatigue, the speed of motion and the electrode position, therefore in the next work, this factors need to be considered.

Ethical approval: “All procedures performed in studies involving human participants were in accordance with the ethical standards of the institutional and/or national research committee and with the 1964 Helsinki declaration and its later amendments or comparable ethical standards.

## REFERENCES

1. Oskoei, M. A. and Hu, H., “Myoelectric Control Systems - A Survey,” Biomedical Signal Processing and Control, Vol. 2, No. 4, pp. 275-294, 2007.
2. Gopura, R., Bandara, D. S. V., Gunasekara, J. M. P., and Jayawardane, T. S. S., “Recent Trends in EMG-Based Control Methods for Assistive Robots,” in: Electrodiagnosis in New Frontiers of Clinical Research, Turker, H., (Ed.), InTech, Chap. 12, 2013.
3. Bai, L., Pepper, M. G., Yana, Y., Spurgeon, S. K., and Sakel, M., “Application of Low Cost Inertial Sensors to Human Motion Analysis,” Proc. of IEEE International Instrumentation and Measurement Technology Conference (I2MTC), pp. 1280-1285, 2012.
4. Hyde, R. A., Ketteringham, L. P., Neild, S. A., and Jones, R. J., “Estimation of Upper-Limb Orientation Based on Accelerometer and Gyroscope Measurements,” IEEE Transactions on Biomedical Engineering, Vol. 55, No. 2, pp. 746-754, 2008.
5. Zhang, Z.-Q., Ji, L.-Y., Huang, Z.-P., and Wu, J.-K., “Adaptive Information Fusion for Human Upper Limb Movement Estimation,” IEEE Transactions on Systems, Man, and Cybernetics-Part A: Systems and Humans, Vol. 42, No. 5, pp. 1100-1108, 2012.
6. Fleischer, C., Kondak, K., Reinicke, C., and Hommel, G., “Motion Calculation for Human Lower Extremities Based on EMG-Signal-Processing and Simple Biomechanical Model,” Climbing and Walking Robots, Armada, M. A., Gonzalez Santos, P., (Eds.), Springer, pp. 153-161, 2005.
7. Fleischer, C., “Controlling Exoskeletons with EMG Signals and a Biomechanical Body Model,” M.Sc. Thesis, Technische Universität Berlin, 2007.
8. Jang, G., Kim, J., Choi, Y., and Yim, J., “Human Shoulder Motion Extraction Using EMG Signals,” Int. J. Precis. Eng. Manuf., Vol. 15, No. 10, pp. 2185-2192, 2014.
9. Tang, Z., Zhang, K., Sun, S., Gao, Z., Zhang, L., and Yang, Z., “An Upper-Limb Power-Assist Exoskeleton Using Proportional Myoelectric Control,” Sensors, Vol. 14, No. 4, pp. 6677-6694, 2014.
10. Doheny, E. P., Lowery, M. M., FitzPatrick, D. P., and O’Malley, M. J., “Effect of Elbow Joint Angle on Force-EMG Relationships in Human Elbow Flexor and Extensor Muscles,” Journal of Electromyography and Kinesiology, Vol. 18, No. 5, pp. 760-770, 2008.
11. Smith, L. H., Hargrove, L. J., Lock, B. A., and Kuiken, T. A., “Determining the Optimal Window Length for Pattern Recognition-Based Myoelectric Control: Balancing the Competing Effects of

Classification Error and Controller Delay," IEEE Transactions on Neural Systems and Rehabilitation Engineering, Vol. 19, No. 2, pp. 186-192, 2011.

12. Momen, K., Krishnan, S., and Chau, T., "Real-Time Classification of Forearm Electromyographic Signals Corresponding to User-Selected Intentional Movements for Multifunction Prosthesis Control," IEEE Transactions on Neural Systems and Rehabilitation Engineering, Vol. 15, No. 4, pp. 535-542, 2007.
13. Fougner, A., Scheme, E., Chan, A. D., Englehart, K., and Stavdahl, Ø., "Resolving the Limb Position Effect in Myoelectric Pattern Recognition," IEEE Transactions on Neural Systems and Rehabilitation Engineering, Vol. 19, No. 6, pp. 644-651, 2011.
14. Artemiadis, P. K. and Kyriakopoulos, K. J., "An EMG-Based Robot Control Scheme Robust to Time-Varying EMG Signal Features," IEEE Transactions on Information Technology in Biomedicine, Vol. 14, No. 3, pp. 582-588, 2010.
15. Kiguchi, K. and Hayashi, Y., "EMG-Based Control of a Lower-Limb Power-Assist Robot," in: Intelligent Assistive Robots, Mohammed, S., Moreno, J., Kong, K., Amirat, Y., (Eds.), Springer Tracts in Advanced Robotics, Vol. 106, pp. 371-383, 2015.
16. Kiguchi, K. and Hayashi, Y., "An EMG-Based Control for an Upper-Limb Power-Assist Exoskeleton Robot," IEEE Transactions on Systems, Man, and Cybernetics, Part B (Cybernetics), Vol. 42, No. 4, pp. 1064-1071, 2012.
17. Oskoei, M. A., and Hu, H., "Support Vector Machine-Based Classification Scheme for Myoelectric Control Applied to Upper Limb," IEEE Transactions on Biomedical Engineering, Vol. 55, No. 8, pp. 1956-1965, 2008.
18. Lenzi, T., De Rossi, S. M. M., Vitiello, N., and Carrozza, M. C., "Intention-Based EMG Control for Powered Exoskeletons," IEEE Transactions on Biomedical Engineering, Vol. 59, No. 8, pp. 2180-2190, 2012.
19. Pau, J. W., Xie, S. S., and Pullan, A. J., "Neuromuscular Interfacing: Establishing an EMG-Driven Model for the Human Elbow Joint," IEEE Transactions on Biomedical Engineering, Vol. 59, No. 9, pp. 2586-2593, 2012.
20. Kuan, J.-Y., Huang, T.-H., and Huang, H.-P., "Human Intention Estimation Method for a New Compliant Rehabilitation and Assistive Robot," Proc. of SICE Annual Conference, pp. 2348-2353, 2010.
21. Ding, Q., Zhao, X., Xiong, A., and Han, J., "A Novel Motion Estimate Method of Human Joint with EMG-Driven Model," Proc. of 5th International Conference on Bioinformatics and Biomedical Engineering, pp. 1-5, 2011.
22. Li, Z., Wang, B., Sun, F., Yang, C., Xie, Q., and Zhang, W., "sEMG-Based Joint Force Control for an Upper-Limb Power-Assist Exoskeleton Robot," IEEE Journal of Biomedical and Health Informatics, Vol. 18, No. 3, pp. 1043-1050, 2014.
23. SENIAM, "Surface ElectroMyoGraphy for the Non-Invasive Assessment of Muscles," http://www.seniam.org/ (Accessed 20 NOV 2017)
24. Martini, F. and Nath, J. L. "Fundamentals of Anatomy & Physiology," Pearson/Benjamin Cummings, San Francisco, pp. 347-359, 2009.
25. Tan, L., "Digital Signal Processing: Fundamentals and Applications," Academic Press, 1st Ed., 2007.
26. Hudgins, B., Parker, P., and Scott, R. N., "A New Strategy for Multifunction Myoelectric Control," IEEE Transactions on Biomedical Engineering, Vol. 40, No. 1, pp. 82-94, 1993.
27. Phinyomark, A., Phukpattaranont, P., and Limsakul, C., "Feature Reduction and Selection for EMG Signal Classification," Expert Systems with Applications, Vol. 39, No. 8, pp. 7420-7431, 2012.
28. Chowdhury, R. H., Reaz, M. B., Ali, M. A. B. M., Bakar, A. A., Chellappan, K., and Chang, T. G., "Surface Electromyography Signal Processing and Classification Techniques," Sensors, Vol. 13, No. 9, pp. 12431-12466, 2013.
29. De Luca, C. J., "Surface Electromyography: Detection and Recording," https://www.delsys.com/Attachments_pdf/WP_SEMGintro.pdf (Accessed 31 OCT 2017)
30. Du, Y.-C., Lin, C.-H., Shyu, L.-Y., and Chen, T., "Portable Hand Motion Classifier for Multi-Channel Surface Electromyography Recognition Using Grey Relational Analysis," Expert Systems with Applications, Vol. 37, No. 6, pp. 4283-4291, 2010.
31. Zardoshti-Kermani, M., Wheeler, B. C., Badie, K., and Hashemi, R. M., "EMG Feature Evaluation for Movement Control of Upper Extremity Prostheses," IEEE Transactions on Rehabilitation Engineering, Vol. 3, No. 4, pp. 324-333, 1995.
32. Kalman, R. E., "A New Approach to Linear Filtering and Prediction Problems," Journal of Basic Engineering, Vol. 82, No. 1, pp. 35-45, 1960.
33. Bishop, G. and Welch, G., "An Introduction to the Kalman Filter," University of North Carolina at Chapel Hill, 1995.
34. Siswantoro, J., Prabuwono, A. S., Abdullah, A., and Idrus, B., "A Linear Model Based on Kalman Filter for Improving Neural Network Classification Performance," Expert Systems with Applications, Vol. 49, pp. 112-122, 2016.
35. Song, R., Tong, K.-y., Hu, X., and Li, L., "Assistive Control System Using Continuous Myoelectric Signal in Robot-Aided Arm Training for Patients after Stroke," IEEE Transactions on Neural Systems and Rehabilitation Engineering, Vol. 16, No. 4, pp. 371-379, 2008.
36. Artemiadis, P. K. and Kyriakopoulos, K. J., "EMG-Based Position and Force Estimates in Coupled Human-Robot Systems: Towards EMG-Controlled Exoskeletons," in: Experimental Robotics, Khatib, O., Kumar, V., Pappas, G. J., (Eds.), Springer Tracts in Advanced Robotics, pp. 241-250, 2009.
37. Kremelberg, D., "Pearson's r, Chi-Square, T-Test, and ANOVA," in: Practical Statistics: A Quick and Easy Guide to IBM SPSS Statistics, STATA, and Other Statistical Software, Kremelberg, D., (Ed.), SAGE,

Chap. 4, 2011.

38. Koo, T. K. and Mak, A. F., "Feasibility of Using EMG Driven Neuromusculoskeletal Model for Prediction of Dynamic Movement of the Elbow," Journal of Electromyography and Kinesiology, Vol. 15, No. 1, pp. 12-26, 2005.
39. Lee, S., Kim, H., Jeong, H., and Kim, J., "Analysis of Musculoskeletal System of Human during Lifting Task with Arm Using Electromyography," Int. J. Precis. Eng. Manuf., Vol. 16, No. 2, pp. 393-398, 2015.
40. Basmajian, J. V. and de Luca, C. J., "Muscle Fatigue and Time-Dependent Parameters of the Surface EMG Signal," in: Muscles Alive: Their Function Revealed by Electromyography, Basmajian, J. V., de Luca, C. J. (Eds.), Williams & Wilkins, pp. 201-222, 1985.